The Journal of Pathology: Clinical Research
J Path: Clin Res April 2018; **4:** 124–134
Published online 24 January 2018 in Wiley Online Library (wileyonlinelibrary.com). DOI: 10.1002/cjp2.97

ORIGINAL ARTICLE

Reduced lymphotoxin-beta production by tumour cells is associated with loss of follicular dendritic cell phenotype and diffuse growth in follicular lymphoma

Giuseppina Pepe†, Arianna Di Napoli†*, Claudia Cippitelli, Stefania Scarpino, Emanuela Pilozzi and Luigi Ruco

Pathology Unit, Department of Clinical and Molecular Medicine, Sapienza University, Sant'Andrea Hospital, Rome, Italy

**Correspondence to: Arianna Di Napoli, Department of Clinical and Molecular Medicine, University Sapienza of Rome, Sant'Andrea Hospital, Via di Grottarossa 1035, 00189 Roma, Italy. E-mail: arianna.dinapoli@uniroma1.it*

†*Contributed equally.*

Abstract

Cytokine production is essential for follicular dendritic cell (FDC) maintenance and organization of germinal centres. In follicular lymphoma, FDCs are often disarrayed and may lack antigens indicative of terminal differentiation. We investigated the *in situ* distribution of cells producing lymphotoxin-beta (*LTB*), lymphotoxin-alpha (*LTA*), and tumour necrosis factor-alpha (*TNFA*) transcripts in human reactive lymph nodes and in follicular lymphomas with follicular or diffuse growth pattern. *LTB* was the cytokine most abundantly produced in germinal centres. *LTB* was present in nearly 90% of germinal centre cells whereas *LTA* and *TNFA* were detected in 30 and 50%, respectively. Moreover, the amount of *LTB* expressed in reactive germinal centre cells was 80-fold higher than that of *LTA* and 20-fold higher than that of *TNFA*. *LTB*-positive cells were more numerous in the germinal centre dark zone, whereas expression of the FDC proteins CD21, CD23, VCAM, and CXCL13 was more intense in the light zone. Tumour cells of follicular lymphomas produced less *LTB* than reactive germinal centre cells. The results of the *in situ* study were confirmed by RT-PCR; *LTB* was significantly more abundant in reactive lymph nodes than in follicular lymphoma, with the lowest values detected in predominantly diffuse follicular lymphoma. In neoplastic follicles, low production of *LTB* by tumour B cells was associated with weaker expression of CD21+/CD23+ by FDCs. Our findings detail for the first time the distribution of *LTA*-, *LTB*-, and *TNFA*-producing cells in human reactive germinal centres and in follicular lymphoma. They suggest the possibility that impaired tumour-cell *LTB* production may represent a determinant of FDC phenotype loss and for defective follicular organization in follicular lymphoma.

Keywords: lymphotoxin-beta lymphotoxin-alpha; TNF-alpha; lymph nodes; lymphoid hyperplasia; follicular lymphoma; follicular dendritic cell; *in situ* hybridization

Received 30 August 2017; Revised 1 January 2018; Accepted 15 January 2018

No conflicts of interest were declared.

Introduction

Organization of B cell follicles requires a mutually dependent collaboration of B cells and follicular dendritic cells (FDCs). While FDCs provide signals to sequester and maintain B cells within B cell follicles (CXCL13), B cells are essential for FDC maintenance by providing stimulation with tumour necrosis factor-alpha (TNFA) and lymphotoxin (LT) [1]. Mature FDCs derive from perivascular mural cells expressing platelet-derived growth factor receptor-beta and alpha smooth muscle actin. Perivascular mural cells also give rise to fibroblastic reticular cells (FRCs) and marginal reticular cells (MRCs) [2]. FDCs, FRCs, and MRCs have distinct morphologies and functions, but share common markers, and are probably strongly correlated [3].

Receptors for LT and TNF (LTβR and TNFR1) are highly expressed on FDC-precursors. Mice deficient in LTβR, TNFR1, or their ligands suffer from complex pathological phenotypes of lymphoid organs which may be devoid of FDCs [4–11]. It is well-established that LT and/or TNFα play a crucial role for maintenance of most FDC traits [12,13]; they

© 2018 The Authors The Journal of Pathology: Clinical Research published by The Pathological Society of Great Britain and Ireland and John Wiley & Sons Ltd

This is an open access article under the terms of the Creative Commons Attribution-NonCommercial-NoDerivs License, which permits use and distribution in any medium, provided the original work is properly cited, the use is non-commercial and no modifications or adaptations are made.

consist of CXCL13 production [14–16], expression of ICAM1, VCAM1, and MadCAM1 [17,18], expression of complement receptors 1 and 2 (CR1 and CR2), and expression of Fc receptors for IgG, IgE, IgA, and IgM [18]. Inhibition of LT leads to the disappearance of multiple markers on FDCs. Inhibition of the TNFα pathway is also effective, but only in the absence of a strong antigenic response.

Most of the information concerning interactions between cytokines and FDCs were obtained in murine models or in *in vitro* studies. Until recently, visualization of cytokine-producing cells in tissue sections was extremely difficult. The development of RNA *in situ* hybridization (ISH) with the RNAscope technology has provided a major advance [19]. In fact, this technology is highly specific, and allows identification of cytokine-producing cells in tissue sections; moreover, the number of cytoplasmic dots per cell represents an approximate quantitative indication of the amount of cytokine RNA.

In the present study, we have investigated the tissue distribution of cells producing lymphotoxin-alpha (*LTA*), lymphotoxin-beta (*LTB*), and *TNFA* RNA in human reactive B cell follicles and in follicular B cell lymphomas (FL). Cytokine production was compared with expression of molecules indicative of FDC differentiation (CD21, CD23, VCAM, and CXCL13). Our findings indicate that there is a strict correlation between *LTB* production and FDC differentiation in reactive follicles and also in FL.

Materials and methods

Patients

Twenty-six lymph nodes, removed for diagnostic purpose at the Sant'Andrea Hospital of Rome, were investigated. Eleven cases (8M:3F; mean age= 58 years) were diagnosed as reactive lymphadenitis (RL) with follicular hyperplasia. Lymph node site was: cervical (two), axillary (four), mediastinal (three), inguinal (one), and supraclavicular (one); the mean size of the lymph nodes was 1.75 cm. Eight cases were diagnosed as follicular lymphoma with predominantly follicular growth pattern (5M:3F), age-range 51–82 years (mean age = 66 years), size range 1.8–3.8 cm (mean size = 2.6 cm). Grading: G1/G2 ($n = 8$). Lymph node site: inguinal ($n = 4$), axillary ($n = 2$), mediastinal ($n = 1$), and cervical ($n = 1$). Seven cases were classified as predominantly diffuse FL (3M:4F) 49–68 years (mean age = 58 years), lymph node size 2.5–4.5 cm (mean = 3.43 cm). Grading: G1/G2 ($n = 7$). Lymph node site: inguinal ($n = 6$), cervical ($n = 1$). The study was performed in accordance with the Helsinki Declaration. Institutional Review Board approval was obtained (EC n° 168/SA/2003).

Tissue samples and immunostaining

Lymph nodes were formalin-fixed and paraffin-embedded (FFPE). Paraffin sections were immunostained for CD21 (clone 1F8), CD23 (clone MHM6), Bcl-2 (clone 124), CD10 (clone 56C6), Ki-67 (clone Mib-1) (Dako, Denmark), Stathmin (clone SP49; Spring Bioscience, Pleasanton, CA USA), VCAM (Clone VCAM1/843; Scytek Laboratories, Logan, UT, USA), and CXCL13 (Polyclonal Goat; R&D Systems, Minneapolis, MA, USA), using an automated immunostainer (Dako). The staining of follicular stroma and interfollicular fibroblastic stroma was graded quantitatively as previously described [20]: 0, absent; 1+ focal; 2+ extensive; 3+ diffuse.

Cytokine production

Cytokine mRNA production was investigated using two different techniques: RNA ISH with RNAscope technology (Advanced Cell Diagnostics, Milano, Italy), and real-time PCR (RT-PCR). RNAscope is an *in situ* enzymatic technique that also provides quantitative information; in fact, the number of dots per cell is directly proportional to the number of specific RNA molecules.

RNAscope

The RNAscope assay was applied to tissue paraffin sections using probes for *LTA*, *LTB*, and *TNFA*, as previously described [19]. In brief, FFPE tissue sections 2 μm thick were deparaffinized in xylene and then hydrated in an ethanol series. Hybridization was with target probes: Probe-Hs-LTA, Probe-Hs-LTB, and Probe-Hs-TNFA. The preamplifier, amplifier, label probe, and chromogenic detection procedures were performed according to the manufacturer's instructions (RNAscope 2.0 HD Reagent Kit, Advanced Cell Diagnostics, Hayward, CA, USA).

RNAscope-stained tissue sections were digitalized at ×40 magnification using Aperio Scan Scope. Digital slides were used for determining percentage of positive cells and pixel of reactivity. For each lymph node, five different areas, measuring 17 000 μm^2 each, were selected within different regions (i.e. GC, mantle, interfollicular). The percentage of positive cells per area was then calculated by manually counting the total number of cells and the number of stained cells directly on the screen. The number of positive pixels was determined using the Aperio software *Positive Pixel Count v9 Algorithm.*

© 2018 The Authors The Journal of Pathology: Clinical Research published by The Pathological Society of Great Britain and Ireland and John Wiley & Sons Ltd

RNA isolation and real-time PCR

Total RNA was extracted from paraffin sections of 25 lymph nodes (11 reactive, 8 nodular follicular lymphoma, and 6 diffuse follicular lymphoma) using High Pure miRNA Isolation kit (Roche Diagnostics, Monza, Italy). The quantity and quality of the RNA was determined using a NanoDrop 2000 spectrophotometer (Thermo Scientific, Waltham, MA USA). One microgram of purified RNA was reverse transcribed into cDNA using iScript Select cDNA Synthesis Kit (BIO-RAD, Milan, Italy) according to the manufacturer's protocol. For cytokine mRNA expression analysis, real-time PCR was performed using QuantiFast SYBR Green PCR Kit (Qiagen, Hilden, Germany) and the expression levels of cytokine were normalized to the housekeeping gene β-actin. Real-time PCR was performed on a 7500 Fast Real-Time PCR System (AB). Primer sequences used for real-time PCR analysis were: *LTB* fwd (5′- GAG GAC TGG TAA CGG AGA CG −3′); *LTB* rev (5′-GGG CTG AGA TCT GTT TCT GG- 3′); *ACTB* fwd (5′-CGG TTC CGC TGC CCT GAG-3′); *ACTB* rev (5′-TGG AGT TGA AGG TAG TTT CGT GGA T-3′). Results of RT-PCR performed in FFPE tissue were expressed as relative levels of *LTB* mRNA in reactive and neoplastic lymph nodes with reference to *LTB* mRNA of a reactive lymph node (RL1) that was chosen to represent 1x expression. Experiments were performed in triplicate.

Combined ISH and immunohistochemistry

RNAscope assay for *LTB* RNA was carried out on a FFPE section from a reactive lymph node as described above. After hybridization slides were immunostained for CD79a (clone JCB117, Dako) using Envision G/2 System/AP, Rabbit/Mouse (Permanent Red) (Agilent, CA, United States) following the manufacturer's instructions. Slides were mounted using Glycergel Mounting Medium (Dako).

Fluorescence *in situ* hybridization (FISH) analyses

Interphase FISH was performed on 2 μm-thick FFPE sections of lymph nodes with a diagnosis of predominantly diffuse follicular lymphoma using dual colour break-apart *BCL-2* probe (Kreatech, Leica Biosystems, Italy), dual colour LSI 1p36/LSI 1q25 probe (Vysis, Abbott, Chicago, USA), and the pretreatment kit (Tissue digestion kit, Kreatech, Leica Biosystems) following the manufacturer's instructions. Sections were then viewed under a NIKON fluorescent microscope with appropriate filters (NIKON Instrument, Italy). The hybridisation signals for each probe were evaluated in at least 100 interphase nuclei.

1p36 loss of heterozygosity (LOH)

1p36 LOH was assessed using five dinucleotide repeats (D1S2734, D1S199, D15508, D1S243, and D1S468). One of the primers in each pair was fluorescently labelled. Data analysis was performed using GeneScan software on a genetic analyzer ABI3I00 (Applied Biosystems, Foster City, CA, USA). Samples were regarded as uninformative if the normal tissue was homozygous or if instability was present in neoplastic tissue. LOH of a locus was determined using the calculation of Ganzian *et al* [21]. Ratios less than 0.6 or greater than 1.67 were regarded as loss of the major or minor allele, respectively.

Statistical analysis

The expression levels of *LTB*, *LTA*, and *TNFA* mRNA assessed by RNAscope or by RT-PCR were compared among the samples using Student's *t*-test.

Results

LTB RNA is produced in B cell follicles of reactive lymph nodes

Cytokines known to be active in FDC differentiation (LTA, LTB, and TNFA) were investigated in paraffin sections of reactive lymph nodes. Cells producing cytokine RNAs were demonstrated with the RNAscope technology. Our findings provide evidence that *LTB* RNA is present mostly in reactive B cell follicles (Figure 1). At that site, cells positive for *LTA* RNA and *TNFA* RNA were significantly less numerous and contained fewer dots of reactivity (Figure 2). A more accurate estimate of the number of cytokine-positive cells was performed on digital slides (Table 1). It was found that almost 90% of GC cells were positive for *LTB* RNA, whereas cells producing *LTA* and/or *TNFA* RNA were significantly less numerous (30 and 50% reduction, respectively; $p \leq 0.001$). This difference was more evident when cytokine RNAs were evaluated as pixels per area; in fact, *LTB* RNA produced by GC cells was 80-fold higher than that of *LTA* and 20-fold higher than that of *TNFA* ($p < 0.001$). These findings indicate that a large proportion of GC B cells are capable of producing *LTA*, *LTB*, and *TNFA*; nevertheless, the amount of *LTB* RNA produced by each single cell is much higher as compared with *LTA* and *TNFA*.

Most RNA-positive cells had the morphology of GC B cells; GC macrophages were negative for *LTA*,

© 2018 The Authors The Journal of Pathology: Clinical Research published by The Pathological Society of Great Britain and Ireland and John Wiley & Sons Ltd

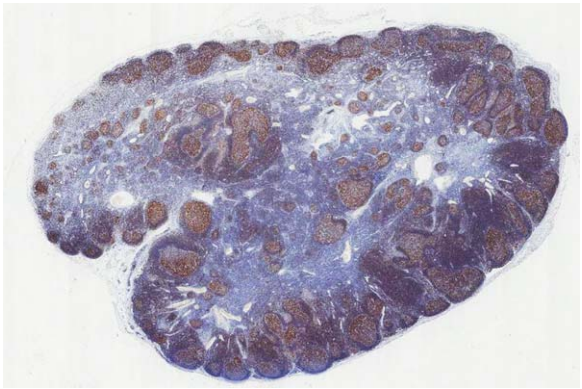

Figure 1. *In situ* hybridization for *LTB* RNA in a reactive lymph node using RNAscope technology. Reactivity, consisting of cytoplasmic brown dots, is present in the cytoplasm of RNA-producing cells, and is directly proportional to the number of RNA molecules. *LTB* RNA was mainly associated with cortical B cell follicles. GCs and mantle zones were both stained with higher levels in GCs.

LTB, and *TNFA*. When GCs were compared with mantle zones, it was found that mantle cells were less efficient than GC cells in producing *LTB* RNA (Table 1). In fact, mantle cells stained for *LTB* RNA were less numerous (76 versus 88%; $p = 0.137$) and produced 40% less *LTB* (81 131 pixels versus 129 372 pixels $p = 0.039$) than GC cells. Mantle cells were also less effective in producing *LTA* RNA (611 pixels versus 1605 pixels $p = 0.009$) and *TNFA* RNA (3306 pixels versus 6633 pixels $p = 0.037$).

The presence of GC cells positive for *LTB* RNA correlated with expression of CD21, CD23, VCAM, and CXCL13 by FDCs (Table 2). As expected, FDCs were diffusely and intensely positive for CD21/CD23, and were focally positive for VCAM and CXCL13. The percentage of GC cells positive for *LTB* RNA varied from 55 to 95% (mean 80 ± 13), and the number of pixels per cell varied from 442 to 1000 (743 ± 231). An interesting observation, made possible by the *in situ* study, was that cells positive for *LTB* RNA were not distributed homogenously throughout the GC. In fact, cells positive for *LTB* RNA were more numerous in the basal dark zone of polarized GCs, where cell proliferation takes place (Figure 3). In contrast, expression of *LTB* induced molecules, such as CD21, CD23, VCAM, and CXCL13 was more prominent in the light zone, proximal to the sub-capsular sinus (Figure 3).

Production of *LTB* RNA in T-dependent interfollicular areas was significantly lower ($p < 0.0001$) as compared with B cell follicles (Table 1). At that site, *LTB*-positive pixels ($17\ 975 \pm 10\ 816$) were 19% of those present in GCs. In Figure 3, a lymph node section was double-stained for *LTB RNA* (brown) and CD79a protein (red). It was confirmed that most *LTB*+ cells were of B cell origin (CD79a+), that they were polarized in GC, and that *LTB*+ cells were much less numerous in CD79a-negative interfollicular T cell areas. Stromal reticular cells of interfollicular areas were negative for CD21/CD23, and were occasionally positive for VCAM/CXCL13.

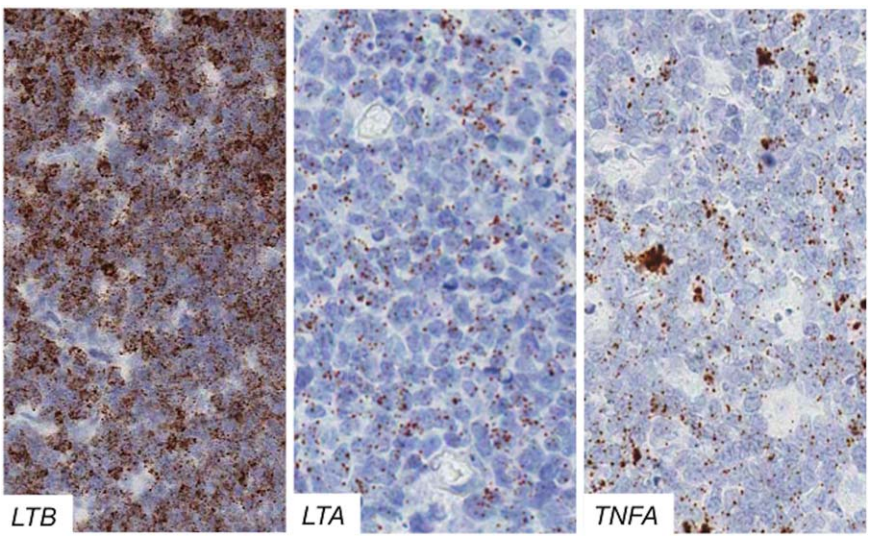

Figure 2. *In situ* hybridization for cytokines in a GC using RNAscope technology. *LTB* RNA (A), *LTA* RNA (B), and *TNFA* RNA (C) were all present, but *LTB* reactivity was much more pronounced. Large cells with clear cytoplasm and tingible bodies (GC macrophages) did not showed reactivity for *TNFA* RNA (C).

© 2018 The Authors The Journal of Pathology: Clinical Research published by The Pathological Society of Great Britain and Ireland and John Wiley & Sons Ltd

Table 1. *LTA* RNA, *LTB* RNA, and *TNFA* RNA in B cell follicles and in interfollicular areas of reactive lymph nodes*

Case No.	*LTA*+ cells (%)	*LTA*+ pixels	*LTB*+ cells (%)	*LTB*+ pixels	*TNFA*+ cells (%)	*TNFA*+ pixels
Germinal centre						
1	23	857 ± 455	83	123 621 ± 50 123	48	7071 ± 3129
2	33	1503 ± 613	93	137 052 ± 64 044	34	2871 ± 1171
3	37	2209 ± 1166	95	140 043 ± 32 107	66	7978 ± 1041
4	30	1849 ± 685	80	116 592 ± 62 562	55	8613 ± 3882
Mean± SD**	**31 ± 6**	**1605 ± 576**	**88 ± 7**	**129 327 ± 11 094**	**51 ± 13**	**6633 ± 2587**
Mantle zone						
1	10	370 ± 376	90	120 847 ± 9834	52	4531 ± 1407
2	16	524 ± 144	90	116 931 ± 43 960	24	1007 ± 328
3	17	863 ± 479	72	51 598 ± 8175	54	4460 ± 1535
4	15	685 ± 333	50	35 149 ± 13 533	33	3227 ± 2394
Mean±SD**	**15 ± 3**	**611 ± 212**	**76 ± 19**	**81 131 ± 44 142**	**41 ± 15**	**3306 ± 1646**
Interfollicular area						
1	14	356 ± 173	75	31 710 ± 10 500	19	2212 ± 774
2	6	519 ± 738	51	17 563 ± 10 677	10	868 ± 269
3	7	945 ± 324	30	5256 ± 4431	13	1156 ± 306
4	13	801 ± 541	41	17 370 ± 12 551	29	4059 ± 3570
Mean±SD**	**10 ± 4**	**655 ± 266**	**49 ± 19**	**17 975 ± 10 816**	**18 ± 8**	**2051 ± 1442**

Statistical analysis (Student *t*-test):
Germinal centre: *LTB*+ cells *versus LTA*+ cells $p < 0.001$; *LTB*+ pixels *versus LTA*+ pixels $p < 0.001$; *LTB*+ cells *versus TNFA*+ cells $p = 0.001$; *LTB*+ pixels *versus TNFA*+ pixels $p < 0.001$; *LTA*+ cells *versus TNFA*+ cells $p = 0.017$; *LTA*+ pixels *versus TNFA*+ pixels $p = 0.005$.
Mantle zone: *LTB*+ cells *versus LTA*+ cells $p < 0.001$; *LTB*+ pixels *versus LTA*+ pixels $p = 0.005$; *LTB*+ cells *versus TNFA*+ cells $p = 0.01$; *LTB*+ pixels *versus TNFA*+ pixels $p = 0.006$; *LTA*+ cells *versus TNFA*+ cells $p = 0.006$; *LTA*+ pixels *versus TNFA*+ pixels $p = 0.009$.
Interfollicular area: *LTB*+ cells *versus LTA*+ cells $p = 0.004$; *LTB*+ pixels *versus LTA*+ pixels $p = 0.009$; *LTB*+ cells *versus TNFA*+ cells $p = 0.01$; *LTB*+ pixels *versus TNFA*+ pixels $p = 0.01$; *LTA*+ cells *versus TNFA*+ cells $p = 0.07$; *LTA*+ pixels *versus TNFA*+ pixels $p = 0.05$.
Germinal Centre *versus* Mantle Zone: *LTA*+ cells $p = 0.001$; *LTA*+ pixels $p = 0.009$; *LTB*+ cells $p = 0.137$, *LTB*+ pixels $p = 0.039$; *TNFA*+ cells $p = 0.176$, *TNFA*+ pixels $p = 0.037$.
Germinal Centre *versus* Interfollicular Area: *LTA*+ cells $p < 0.001$; *LTA*+ pixels $p = 0.012$; *LTB*+ cells $p = 0.005$, *LTB*+ pixels $p < 0.001$; *TNFA*+ cells $p = 0.003$, *TNFA*+ pixels $p = 0.01$.
Mantle Zone versus Interfollicular Area: *LTA*+ cells $p = 0.065$; *LTA*+ pixels $p = 0.40$; *LTB*+ cells $p = 0.05$, *LTB*+ pixels $p = 0.016$; *TNFA*+ cells $p = 0.017$, *TNFA*+ pixels $p = 0.15$.
*Paraffin sections of four reactive lymph nodes were stained for *LTA, LTB, TNFA* RNA using RNA scope technology. Stained sections were digitalized using Aperio ScanScope. Percentage of stained cells and number of pixels (*Aperio Positive Pixel Count v9 algorithm)* were determined in areas measuring 17 000 μm^2 each. The value reported in the Table is the mean ± SD of five different measurements made in different follicles or in different regions of the same lymph node.
**Mean ± SD of the four investigated cases.

LTB RNA production in B cell follicular lymphomas

Follicular B cell lymphomas are GC-derived malignant tumours, which may exhibit a *follicular* or a *diffuse* pattern of growth. The so-called 'classical-type' FL carries the t(14;18) translocation, expresses BCL2 protein in most cases, and generally has a

Table 2. Immunophenotype of FDCs and *LTB* RNA in germinal centres of reactive lymph nodes

		FDC immunophenotype				*LTB* RNA		
Case No.	Age/sex	CD21	CD23	VCAM	CXCL13	+ cells (%)	+ pixels (*n*)	pixels/cell (*n*)
1	77/M	3+°	3+	3+	1+	83*	123 621 ± 50 123*	902**
2	43/M	3+	3+	1+	2+	78	61 841 ± 14 070	476
3	73/M	2+	2+	1+	1+	93	137 052 ± 64 044	1000
4	32/F	3+	3+	1+	1+	55	38 540 ± 24 996	602
5	81/M	3+	3+	2+	ND	ND	ND	ND
6	74/M	3+	2+	2+	1+	83	61 929 ± 22 160	442
7	63/F	3+	3+	1+	2+	ND	ND	ND
8	77/F	3+	3+	2+	2+	71	63 679 ± 16 271	624
9	71/M	3+	3+	2+	3+	ND	ND	ND
10	8/M	3+	3+	2+	2+	95	140 043 ± 32 107	909
11	34/M	3+	3+	2+	3+	80	116 592 ± 62 562	988
Mean±SD		**2.9 ± 0.3**	**2.8 ± 0.4**	**1.7 ± 0.6**	**1.8 ± 0.8**	**80 ± 13**	**92 912 ± 40 373**	**743 ± 231**

°The immunostaining of FDCs was graded as previously described [20]: absent (0); focal (1+); extensive (2+); diffuse (3+).
*Mean percentage of *LTB*+ cells and mean number of *LTB*+ pixels (*Aperio Positive Pixel Count v9 algorithm)* determined in five different GC areas measuring 17 000 μm^2 each.
**Pixels per cell were calculated as total positive pixels/total number of stained cells.

© 2018 The Authors The Journal of Pathology: Clinical Research published by The Pathological Society of Great Britain and Ireland and John Wiley & Sons Ltd

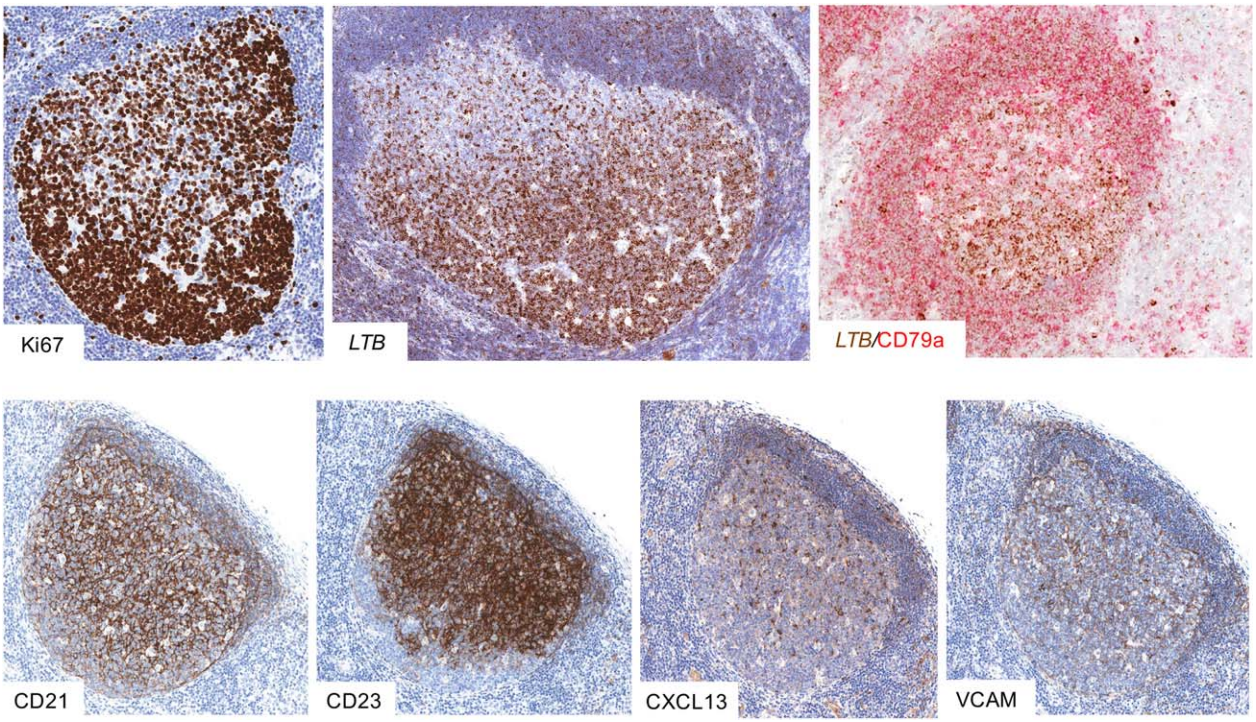

Figure 3. Polarized germinal centre in a reactive lymph node. Cell proliferation (Ki67) and dots of *LTB* RNA (ISH with RNAscope technology) were more evident in the basal dark zone. Combined *in situ* hybridization for *LTB* RNA (brown) and immunohistochemistry for CD79a (red) showed that most *LTB* reactivity is associated with CD79a+ B cells of the mantle and GC dark zone. Very few LTB+ cells were present in the CD79a-negative interfollicular area. Immunostainings for CD21, CD23, CXCL13, and VCAM-1 were more intense in the upper part of the GC facing the sub-capsular sinus.

predominantly follicular pattern of growth. Classical FL with a diffuse pattern of growth is extremely rare. More recently, a distinct subtype of FL has been described, the so-called 'inguinal-type' [22]. The latter is characterized by a predominantly diffuse pattern of growth, is usually BCL2-negative, and often carries the 1p36 deletion. In Table 3, we have investigated *LTB* RNA in *follicular versus diffuse* FL. It was found that tumour cells of predominantly follicular FL were less effective in producing *LTB* RNA than GC cells, but were more efficient than tumour cells of predominantly diffuse FL. In fact, the percentage of *LTB*+ cells in predominantly follicular FL (62%) and the number of *LTB*+ pixels were significantly lower than those of reactive GCs ($p = 0.004$ and $p = 0.001$). In predominantly diffuse FL, the levels of *LTB* RNA were the lowest; in fact, *LTB*+ cells were 14% and *LTB*+ pixels were 3.540 (96% less than GC and 91% less than predominantly follicular FL; $p < 0.001$) (Figure 4). In our series, no correlation was found between *LTB* production and tumour grade (G1/G2) or cell proliferation (% of Ki67+ cells).

Predominantly diffuse FL may still have limited follicular areas. Production of cytokine RNAs was investigated in follicular and diffuse areas of four cases of FL 'inguinal-type' (Table 4). It was found that production of *LTB* RNA was only three-fold higher in follicles as compared to diffuse areas. It is of interest that the small tumour-associated follicles were positive for CD10, BCL-6, and stathmin, but were negative or weakly positive for CD21 and CD23 (Figure 5). These findings seem to indicate that terminal differentiation of FDCs in the follicles of diffuse FL is to some extent impaired.

The data obtained with RNAscope technology indicate that there are significant differences in the levels of *LTB* RNA produced in reactive GCs, predominantly follicular FL and in predominantly diffuse FL. This observation was confirmed by the use of RT-PCR. cDNAs obtained from total RNA extracted from tissue sections of 11 reactive lymph nodes, 8 follicular FLs, and 6 diffuse FLs was tested for the presence of *LTB* by RT-PCR. The data shown in Figure 6 confirm that *LTB* RNA is more abundant in reactive lymph nodes than in predominantly follicular

© 2018 The Authors The Journal of Pathology: Clinical Research published by The Pathological Society of Great Britain and Ireland and John Wiley & Sons Ltd

Table 3. *LTB* RNA and FDCs in predominantly follicular and in predominantly diffuse follicular B cell lymphoma*

Case N.	Age/sex	Lymph node site	Size (cm)	Grade	Ki67 (%)	BCL2#	1p36 loss°	*LTB*+ cells (%)	*LTB*+ pixels	*LTB* pixels/cell
Predominantly follicular FL										
1	51/F	Inguinal	1.8	G2	10	+	ND	54	21 886 ± 11 138	257
2	53/M	Axillary	2.5	G2	40	+	ND	64	33 159 ± 22 146	299
3	67/F	Inguinal	2.5	G1	20	+	ND	75	60 813 ± 13 500	760
4	80/M	Inguinal	3.8	G2	30	-	ND	68	62 476 ± 40 999	625
5	54/M	Cervical	3.0	G2	20	+	ND	40	33 437 ± 9052	423
6	82/M	Mediastinal	2.2	G1	<10	+	ND	68	35 017 ± 11 228	294
7	68/F	Axillary	2.5	G2	10	+	ND	65	28 890 ± 14 113	251
8	70/M	Inguinal	2.5	G2	20	+	ND	58	30 260 ± 8256	309
Mean ± SD								**62 ± 11**	**38 242 ± 14 999**	**402 ± 190**
Predominantly diffuse FL										
1	53/M	Inguinal	3.0	G1	<10	–	+	27	8044 ± 5832	223
2	68/F	Inguinal	3.5	G2	<10	–	+	5	1512 ± 814	252
3	64/M	Inguinal	3.5	G2	20	–	+	5	730 ± 370	146
4	56/M	Cervical	2.5	G2	30	+	ND	5	750 ± 250	125
5	49/F	Inguinal	2.5	G2	10	–	-	33	9072 ± 5412	171
6	51/F	Inguinal	4.5	G2	30	–	+	9	2086 ± 840	116
7	68/F	Inguinal	4.5	G2	<10	–	+	13	2587 ± 456	108
Mean ± SD								**14 ± 12**	**3540 ± 3505**	**163 ± 56**
Reactive lymph nodes (n = 8)^										
Mean ± SD								**80 ± 13**	**92 912 ± 40 373**	**743 ± 231**

Statistical analysis (Student t-Test): RL *versus* follicular FL: *LTB*+ cells $p = 0.004$; *LTB*+ pixels $p = 0.001$; *LTB*+ pixels/cell $p = 0.003$; RL *versus* diffuse FL: *LTB*+ cells $p < 0.001$; *LTB*+ pixels $p < 0.001$; *LTB*+ pixels/cell $p < 0.001$; follicular FL *versus* diffuse FL: *LTB*+ cells $p < 0.001$; *LTB*+ pixels $p < 0.001$; *LTB*+ pixels/cell $p = 0.003$.

*Paraffin sections were stained for *LTB* RNA using RNA scope technology. Stained sections were digitalized using Aperio ScanScope. The percentage of *LTB*+ cells and the mean number of *LTB* pixels were determined in five squared areas measuring 17 000 μm^2 each. Pixels per cell were calculated as total positive pixels/total positive number of stained cells.

#BCL2 expression was investigated by immunohistochemistry, using Dako clone 124. BCL2-negative cases were re-investigated by FISH which confirmed the absence of t(14;18).

°Chromosomal 1p36 loss was investigated by FISH and by LOH analyses.

^Cases are detailed in Table 2.

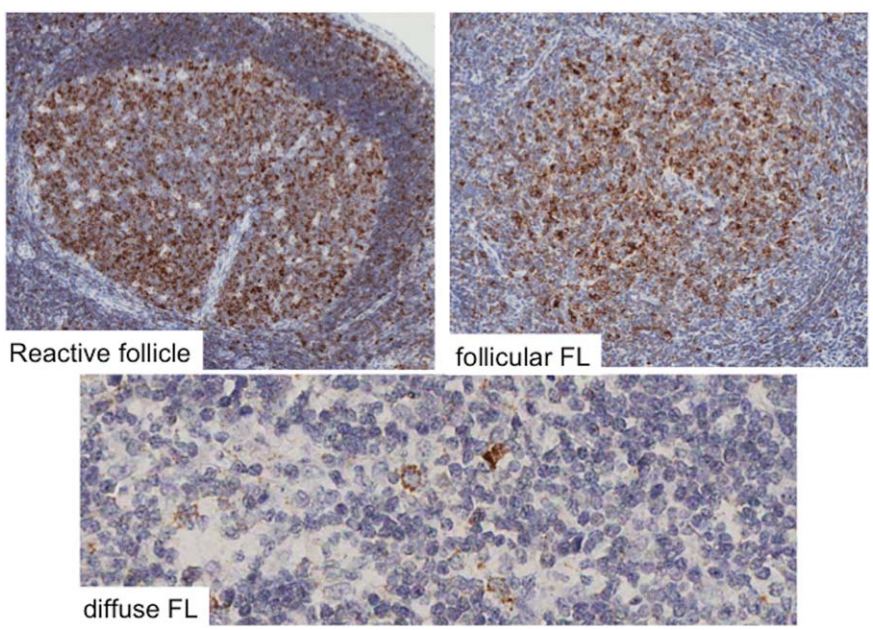

Figure 4. *In situ* hybridization for *LTB* RNA using RNAscope technology in reactive GC, predominantly follicular FL, and predominantly diffuse FL. In reactive follicles, most GC B cells and mantle zone cells are positive for LTB RNA. In follicular FL, most tumour cells are positive. In diffuse FL, only rare cells are stained.

© 2018 The Authors The Journal of Pathology: Clinical Research published by The Pathological Society of Great Britain and Ireland and John Wiley & Sons Ltd

Table 4. *LTB* RNA and CD21/CD23 expression in follicular and diffuse areas of follicular lymphoma*

Case No.	CD21	CD23	*LTB*+ pixels	CD21	CD23	*LTB*+ pixels
			Predominantly follicular FL			
		Follicles			Interfollicular areas	
1	1+	2+	21 886 ± 11 138**	0	0	22 342 ± 8276**
2	3+	2+	33 159 ± 22 146	0	0	2207 ± 1170
3	3+	NE	60 813 ± 13 500	0	NE	7096 ± 6411
4	3+	0	62 476 ± 40 999	NE	1+	17 159 ± 4409
5	2+	NE	33 437 ± 9052	0	NE	16 017 ± 3563
6	3+	1+	35 017 ± 11 228	1+	1+	2748 ± 1543
7	1+	0	28 890 ± 14 113	0	1+	11 305 ± 2497
8	3+	2+	30 260 ± 8256	0	0	5148 ± 2012
Mean ± SD	**2.37 ± 0.92**	**1.17 ± 0.98**	**38 242 ± 14 999**	**0.14 ± 0.38**	**0.50 ± 0.55**	**10 503 ± 7414**
			Predominantly diffuse FL			
		Follicles			Diffuse areas	
1	1+	0	26 539 ± 7794**	1+	NE	8044 ± 5832**
2	1+	1+	7894 ± 14 189	0	0	1512 ± 814
3	0	0	2100 ± 1374	0	1+	730 ± 370
4	1+	0	ND	1+	0	750 ± 250°
5	0	0	25157 ± 3924	0	NE	9072 ± 5412
6	1+	0	ND	1+	NE	2086 ± 840°
7	0	NE	ND	0	NE	2587 ± 456°
Mean ± SD	**0.57 ± 0.53**	**0.17 ± 0.41**	**15 422 ± 12 281**	**0.43 ± 0.53**	**0.33 ± 0.58**	**3540 ± 3505**

Statistical analysis (Student *t*-test):
Follicles *versus* interfollicular area of predominantly follicular FL: CD21 $p < 0.001$; CD23 $p = 0.09$; *LTB*+ pixels $p < 0.001$; Follicles *versus* diffuse areas of predominantly diffuse FL: CD21 $p = 0.31$; CD23 $p = 0.31$; *LTB*+ pixels $p = 0.08$; Follicles of predominantly follicular FL *versus* follicles of predominantly diffuse FL: CD21 $p < 0.001$; CD23 $p = 0.02$; *LTB*+ pixels $p = 0.01$; Interfollicular area of predominantly follicular FL versus interfollicular area of predominantly diffuse FL: CD21 $p = 0.13$; CD23 $p = 0.34$; *LTB*+ pixels $p = 0.02$.
NE, not evaluable because CD21 or CD23 were expressed by the lymphoid component of the tumour as well; ND, not determined.
*Paraffin sections were immunostained for CD21 and CD23. The staining intensity of FDCs was graded quantitatively as previously described [20]: absent (0); focal (1+); extensive (2+); diffuse (3+).
**Paraffin sections were stained for *LTB* RNA using RNA scope technology. Stained sections were digitalized using Aperio ScanScope. The mean numbers of *LTB*+ pixels were determined in five squared areas measuring 17 000 μm^2 each.
°These values were excluded when follicles and diffuse areas were compared in predominantly diffuse FL.

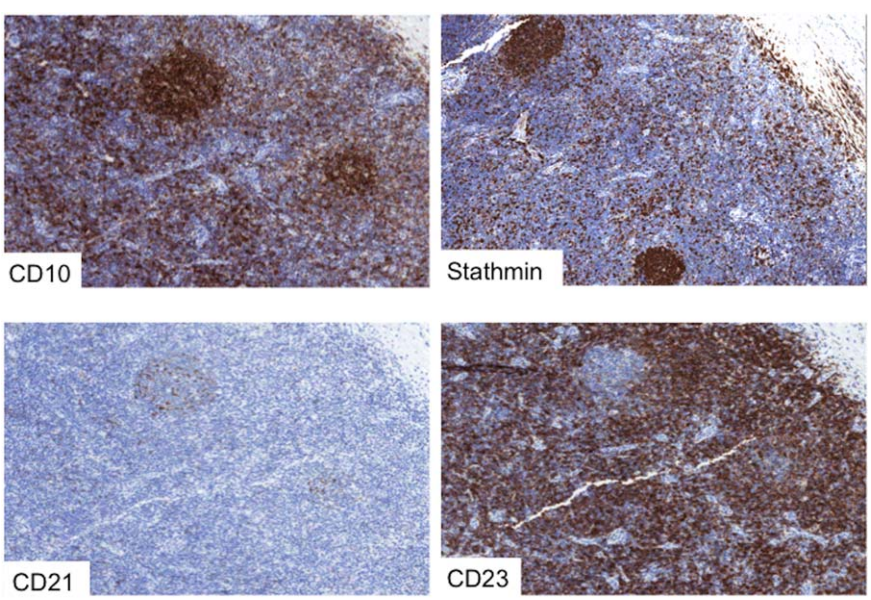

Figure 5. Predominantly diffuse CD23+ B cell FL. Small CD10+/Stathmin+ B cell follicles are poorly stained for CD21/CD23. A positive control is provided by CD23 staining of tumour cells.

© 2018 The Authors The Journal of Pathology: Clinical Research published by The Pathological Society of Great Britain and Ireland and John Wiley & Sons Ltd

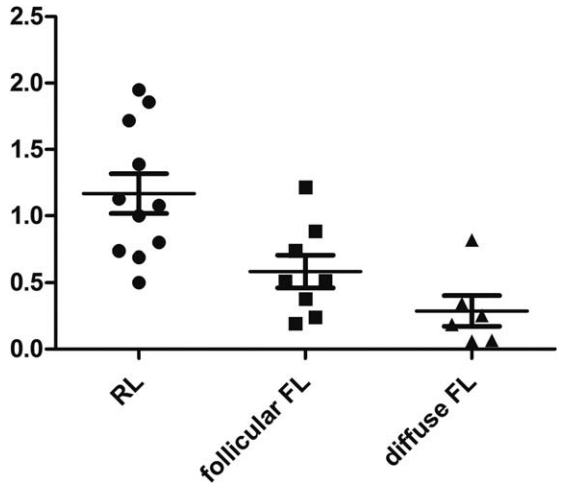

Figure 6. *LTB* RNA expression determined by RT-PCR. Total RNA was extracted from FFPE lymph nodes involved by RL ($n = 11$), predominantly follicular FL ($n = 8$), and predominantly diffuse FL ($n = 6$). Statistical analysis (Student's *t*-test): RL versus follicular FL $p = 0.006$; RL versus diffuse FL $p < 0.001$; follicular FL versus diffuse FL $p = 0.06$.

FL ($p = 0.006$). The lowest values of *LTB* RNA were observed in predominantly diffuse FL (RL *versus* diffuse FL $p < 0.001$), thus confirming the data obtained with ISH.

Discussion

This is the first report describing the tissue distribution of cells producing *LT* and *TNFA* RNA in human lymphoid tissues. Our results show that cells producing *LTB* are mainly located in B cell follicles, and are more numerous than those producing *LTA* and *TNFA*. These observations are consistent with the notion that production of *LTB* RNA is constitutive in B-cells [23,24], whereas production of *LTA* and *TNFA* RNA is inducible [25]. It has to be emphasized that quantitative differences in cytokine RNAs do not necessarily reflect protein synthesis and release. In fact, it has been reported that *TNFA* RNA accumulates rapidly, but has a brief half-life. In contrast, *LTA* RNA accumulates more slowly, but persists much longer with a half-life longer than that of *TNFA* RNA [26]. Thus, RNA half-time and protein translation represent further regulatory checkpoints which might profoundly alter the levels of cytokine production in lymphoid tissues.

We provide evidence that proliferating B cells located in the basal dark zone of GCs contain large amounts of *LTB* RNA, and that light zone FDCs express high levels of molecules involved in FDC function. Indeed, differences in FDCs populating dark and light zone have already been reported. It was described that FDCs in the dark zone were half as dense as FDCs in the light zone [27], and that dark zone FDCs produce large amounts of CXCL12 [28]. These findings and our observations raise the possibility that the topographical organization of GCs in dark and light zones also affects FDC differentiation and function. In fact, B cell proliferation in the dark zone represents a signal that GC cells are efficiently stimulated and that productive antigen presentation is occurring. In this situation, it is necessary to optimize FDC function through induction of molecules involved in antigen trapping (CD21, CD23), cell-cell adhesion (VCAM), and B cell recruitment (CXCL13). Release of high levels of LTB by proliferating B cells of the dark zone might have this role. In agreement with this view, Mackay *et al* [7,12] demonstrated that inhibition of LTA/B in tissue cultures caused disappearance of multiple markers on FDCs within 1 day, and that inhibition of the TNF pathway was much less effective. The possibility that TNF and LT exert different actions on stromal cells is supported by an *in vitro* study [29] showing that TNF alone was able to induce a strong increase of adhesion molecules, but not of meshwork formation, whereas LT had the opposite effect. Thus, it seems likely that LT and TNF are both necessary to support FDC function, but with different roles.

Tumour B cells of predominantly follicular FL show a strict topographical and functional relationship with FDCs [30]; in fact, the latter are crucial for supporting tumour growth and survival [31,32]. Chang *et al* [20] investigated the immunophenotype of FDCs present in FL and found different patterns of antigen expression, depending on the pattern of growth (follicular versus diffuse). They reported that stromal reticular cells of diffuse FL showed only minimal immunophenotypic evidence of FDC-like differentiation, and that FDCs of follicular FL were characterized by reduced expression of FDC antigens as compared to reactive GC. Similar findings were reported in a more recent study, where it was shown that FDCs found in different types of lymphoma show reduced expression of several FDC antigens as compared with normal GCs [33]. We have confirmed and extended these observations. Moreover, the new information provided by our study is that there is a correlation between amounts of *LTB* RNA produced by tumour cells and levels of FDC differentiation of tumour-associated stromal reticular cells.

A purely diffuse pattern is rare in FL. More recently, a peculiar type of diffuse FL was proposed

© 2018 The Authors The Journal of Pathology: Clinical Research published by The Pathological Society of Great Britain and Ireland and John Wiley & Sons Ltd

as a separate entity [22,34,35]. This tumour, known as 'inguinal-type', has distinctive traits consisting of frequent involvement of inguinal lymph nodes, absence of *BCL2* translocation, frequent occurrence of 1p36 deletion, frequent expression of CD23 by tumour B cells, and a better prognosis [22,34,35]. Five of the seven cases of diffuse FL investigated in the present study had features of the 'inguinal-type' variant. We have found that these tumours produce low amounts of *LTB* RNA as compared with 'classical' predominantly follicular FL. It can be speculated that poor production of LTB by tumour cells of predominantly diffuse FL is responsible for defective differentiation of stromal reticular cells into FDCs, and hence for defective nodular organization.

Acknowledgements

This work was supported by a grant from Sapienza University.

Author contributions statement

LR and ADN conceived experiments and designed the study. GP, CC, and SS carried out experiments. ADN, GP, LR, and EP analysed data. LR, ADN, and GP interpreted results and wrote the paper. All authors had final approval of the submitted and published versions.

References

1. Aguzzi A, Kranich J, Krautler NJ. Follicular dendritic cells: origin, phenotype, and function in health and disease. *Trends Immunol* 2014; **35:** 105–113.
2. Krautler NJ, Kana V, Kranich J, *et al*. Follicular dendritic cells emerge from ubiquitous perivascular precursors. *Cell* 2012; **150:** 194–206.
3. Koning JJ, Mebius RE. Interdependence of stromal and immune cells for lymph node function. *Trends Immunol* 2012; **33:** 264–267.
4. Banks TA, Rouse BT, Kerley MK, *et al*. Lymphotoxin-alpha-deficient mice. Effects on secondary lymphoid organ development and humoral immune responsiveness. *J Immunol* 1995; **155:** 1685–1693.
5. Le Hir M, Bluethmann H, Kosco-Vilbois MH, *et al*. Differentiation of follicular dendritic cells and full antibody responses require tumor necrosis factor receptor-1 signaling. *J Exp Med* 1996; **183:** 2367–2372.
6. Alimzhanov MB, Kuprash DV, Kosco-Vilbois MH, *et al*. Abnormal development of secondary lymphoid tissues in lymphotoxin beta-deficient mice. *Proc Natl Acad Sci U S A* 1997; **94:** 9302–9307.
7. Mackay F, Majeau GR, Lawton P, *et al*. Lymphotoxin but not tumor necrosis factor functions to maintain splenic architecture and humoral responsiveness in adult mice. *Eur J Immunol* 1997; **27:** 2033–2042.
8. Tumanov AV, Kuprash DV, Lagarkova MA, *et al*. Distinct role of surface lymphotoxin expressed by B cells in the organization of secondary lymphoid tissues. *Immunity* 2002; **17:** 239–250.
9. Gonzalez M, Mackay F, Browning JL, *et al*. The sequential role of lymphotoxin and B cells in the development of splenic follicles. *J Exp Med* 1998; **187:** 997–1007.
10. Endres R, Alimzhanov MB, Plitz T, *et al*. Mature follicular dendritic cell networks depend on expression of lymphotoxin β receptor by radioresistant stromal cells and of lymphotoxin β and tumor necrosis factor by B cells. *J Exp Med* 1999; **189:** 159–168.
11. Junt T, Tumanov AV, Harris N, *et al*. Expression of lymphotoxin beta governs immunity at two distinct levels. *Eur J Immunol* 2006; **36:** 2061–2075.
12. Mackay F, Browning JL. Turning off follicular dendritic cells. *Nature* 1998; **395:** 26–27.
13. Husson H, Lugli SM, Ghia P, *et al*. Functional effects of TNF and lymphotoxin alpha1beta2 on FDC-like cells. *Cell Immunol* 2000; **203:** 134–143.
14. Ngo VN, Korner H, Gunn MD, *et al*. Lymphotoxin-alpha/beta and tumor necrosis factor are required for stromal cell expression of homing chemokines in B and T cell areas of the spleen. *J Exp Med* 1999; **189:** 403–412.
15. Ansel KM, Ngo VN, Hyman PL, *et al*. A chemokine-driven positive feedback loop organizes lymphoid follicles. *Nature* 2000; **406:** 309–314.
16. Aguzzi A, Krautler NJ. Characterizing follicular dendritic cells: a progress report. *Eur J Immunol* 2010; **40:** 2134.
17. Ware CF. Network communications: lymphotoxins, LIGHT, and TNF. *Annu Rev Immunol* 2005; **23:** 787–819.
18. Myers RC, King RG, Carter RH, *et al*. Lymphotoxin α1β2 expression on B cells is required for follicular dendritic cell activation during the germinal center response. *Eur J Immunol* 2013; **43:** 348–359.
19. Wang F, Flanagan J, Su N, *et al*. RNAscope: a novel in situ RNA analysis platform for formalin-fixed, paraffin-embedded tissues. *J Mol Diagn* 2012; **14:** 22–29.
20. Chang K-C, Huang X, Medeiros LJ, *et al*. Germinal centre-like versus undifferentiated stromal immunophenotypes in follicular lymphoma. *J Pathol* 2003; **201:** 404–412.
21. Canzian F, Salovaara R, Heinminki A, *et al*. Semiautomated assessment of loss of heterozygosity and replication error in tumours. *Cancer Res* 1996; **56:** 3331–3337.
22. Katzenberger T, Kalla J, Leich E, *et al*. A distinctive subtype of t(14;18)-negative nodal follicular non-Hodgkin lymphoma characterized by a predominantly diffuse growth pattern and deletions in the chromosomal region 1p36. *Blood* 2008; **113:** 1053–1061.
23. Worm M, Geha RS. CD40 ligation induces lymphotoxin alpha gene expression in human B cells. *Int Immunol* 1994; **6:** 1883–1890.
24. Pokholok DK, Maroulakou IG, Kuprash DV, *et al*. Cloning and expression analysis of the murine lymphotoxin beta gene. *Proc Natl Acad Sci U S A* 1995; **92:** 674–678.
25. Browning JL, Ngam-Ek A, Lawton P, *et al*. Lymphotoxin beta, a novel member of the TNF family that forms a heteromeric complex with lymphotoxin on the cell surface. *Cell* 1993; **72:** 847–856.

© 2018 The Authors The Journal of Pathology: Clinical Research published by The Pathological Society of Great Britain and Ireland and John Wiley & Sons Ltd

26. English BK, Weaver WM, Wilson CB. Differential regulation of lymphotoxin and tumor necrosis factor genes in human T lymphocytes. *J Biol Chem* 1991; **266:** 7108–7113.
27. Rademakers LH. Dark and light zones of germinal centres of the human tonsil: an ultrastructural study with emphasis on heterogeneity of follicular dendritic cells. *Cell Tissue Res* 1992; **269:** 359–368.
28. Rodda LB, Bannard O, Ludewig B, *et al*. Phenotypic and morphological properties of germinal center dark zone *Cxcl12*-expressing reticular cells (CRCs). *J Immunol* 2015; **195:** 4781–4791.
29. Amé-Thomas P, Maby-El Hajjami H, Monvoisin C, *et al*. Human mesenchymal stem cells isolated from bone marrow and lymphoid organs support tumor B-cell growth: role of stromal cells in follicular lymphoma pathogenesis. *Blood* 2007; **109:** 693–702.
30. Carbone A, Gloghini A. Follicular dendritic cell pattern in early lymphomas involving follicles. *Adv Anat Pathol* 2014; **21:** 260–269.
31. El Shikh ME, Pitzalis C. Follicular dendritic cells in health and disease. *Front Immunol* 2012; **3:** 292.
32. Kridel R, Sehn LH, Gascoyne RD. Pathogenesis of follicular lymphoma. *J Clin Invest* 2012; **122:** 3424–3431.
33. Jin MK, Hoster E, Dreyling M, *et al*. Follicular dendritic cells in follicular lymphoma and types of non-Hodgkin lymphoma show reduced expression of CD23, CD35 and CD54 but no association with clinical outcome. *Histopathology* 2011; **58:** 586–592.
34. Siddiqi IN, Friedman J, Barry-Holson KQ, *et al*. Characterization of a variant of t(14;18) negative nodal diffuse follicular lymphoma with CD23 expression, 1p36/TNFRSF14 abnormalities, and STAT6 mutations. *Mod Pathol* 2016; **29:** 570–581.
35. Swerdlow SH, Campo E, Pileri SA, *et al*. The 2016 revision of the World Health Organization classification of lymphoid neoplasms. *Blood* 2016; **127:** 2375–2390.

© 2018 The Authors The Journal of Pathology: Clinical Research published by The Pathological Society of Great Britain and Ireland and John Wiley & Sons Ltd